**Efferent vagal nerve stimulation protects heart against ischemia-induced arrhythmias by preserving connexin 43 protein.** *Circulation* 112: 164-170

20. Kakinuma Y, Ando M, Kuwabara M, Katare RG, Okudela K, Kobayashi M, Sato T (2005) **Acetylcholine from vagal stimulation protects cardiomyocytes against ischemia and hypoxia involving additive non-hypoxic induction of HIF-1alpha.** *FEBS Lett* 579: 2111-2118

21. Wang H, Yu M, Ochani M, Amella CA, Tanovic M, Susarla S, Li JH, Wang H, Yang H, Ulloa L, Al-Abed Y, Czura CJ, Tracey KJ (2003) **Nicotinic acetylcholine receptor alpha7 subunit is an essential regulator of inflammation.** *Nature* 421: 384-388

22. Du XJ, Cox HS, Dart AM, Esler MD (1998) **Depression of efferent parasympathetic control of heart rate in rats with myocardial infarction: effect of losartan.** *J Cardiovasc Pharmacol* 31: 937-944

23. Bibevski S, Dunlap ME (1999) **Ganglionic mechanisms contribute to diminished vagal control in heart failure.** *Circulation* 99: 2958-2963

24. La Rovere MT, Bigger JT Jr, Marcus FI, Mortara A, Schwartz PJ (1998) **Baroreflex sensitivity and heart-rate variability in prediction of total cardiac mortality after myocardial infarction. ATRAMI (Autonomic Tone and Reflexes After Myocardial Infarction) Investigators.** *Lancet* 351: 478-484

25. La Rovere MT, Pinna GD, Hohnloser SH, Marcus FI, Mortara A, Nohara R, Bigger JT Jr, Camm AJ, Schwartz PJ; ATRAMI Investigators (2001) **Baroreflex sensitivity and heart rate variability in the identification of patients at risk for**

**life-threatening arrhythmias: implications for clinical trials.** *Circulation* 103: 2072-2077

## Figure legends

### Figure 1.

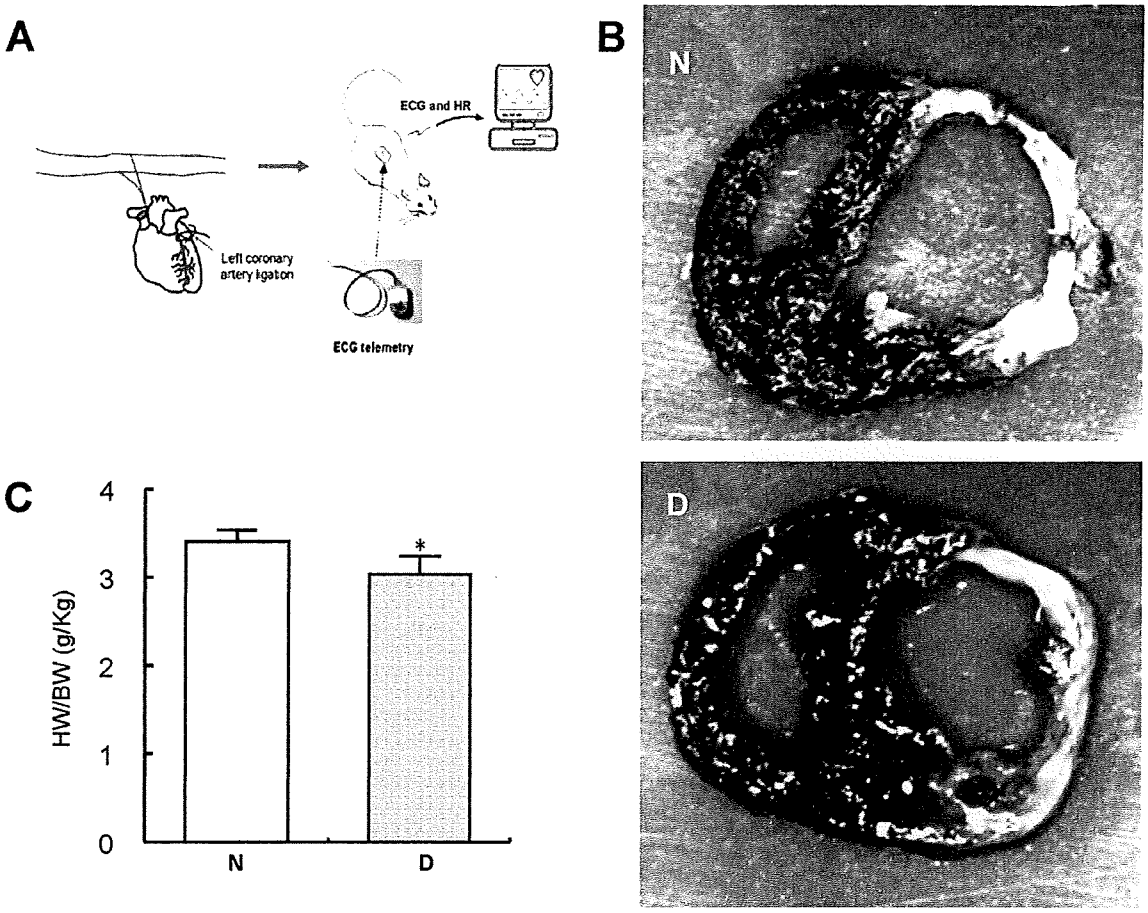


**A:** Schematic representation of the experimental design. Electrocardiogram was recorded continuously using a telemetric system. **B:** Ventricular sections of representative animals at week 6 of treatment. No significant difference in the size of myocardial infarction is observed between the donepezil group and the nontreated group. Compared with the nontreated heart (N), the donepezil-treated heart (D) showed thicker scar in the infarct area with more spared myocardium in the border area. **C:** Combined weight of left and right ventricles per body weight (HW/BW) at week 6 of treatment. Ventricular weight was significantly lower in the donepezil group (shaded bar, D) compared to the nontreated group (open bar, N). *: $p<0.05$

**Figure 2.**

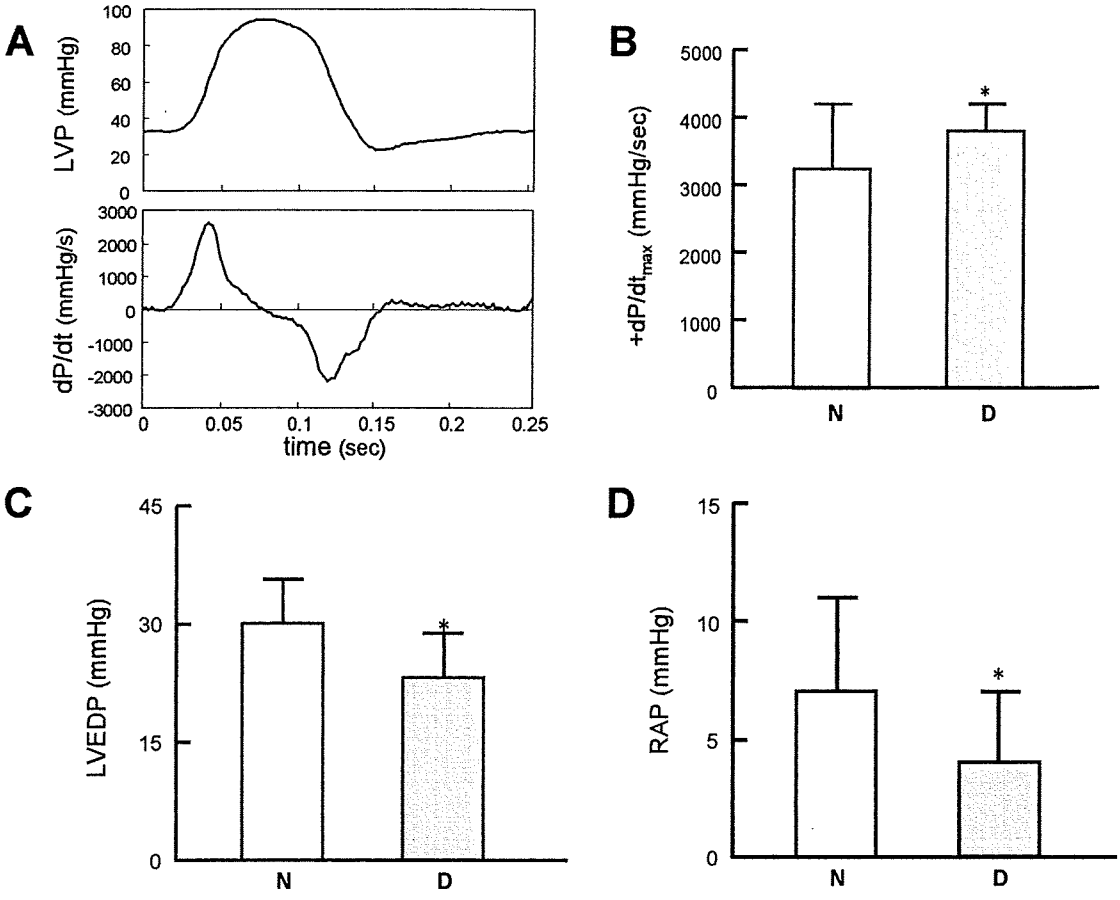


**A:** A representative example of left ventricular pressure waveform and its derivative in a nontreated rat. **B:** Maximal first derivative of left ventricular pressure ($dP/dt_{max}$) at week 6 of treatment. A significant increase in $dP/dt_{max}$ was observed in the donepezil group (shaded bar, D) compared to the nontreated group (open bar, N). *: $p<0.05$ **C:** Left ventricular enddiastolic pressure (LVEDP) at week 6 of treatment. A significant decrease in LVEDP was observed in the donepezil group (shaded bar, D) compared to the nontreated control group (open bar, N). *: $p<0.05$ **D:** Right atrial pressure (RAP) at week 6 of treatment. A significant decrease in RAP was observed in the donepezil group (shaded bar, D) compared to the nontreated control group (open bar, N). *: $p<0.05$

**Figure 3.**

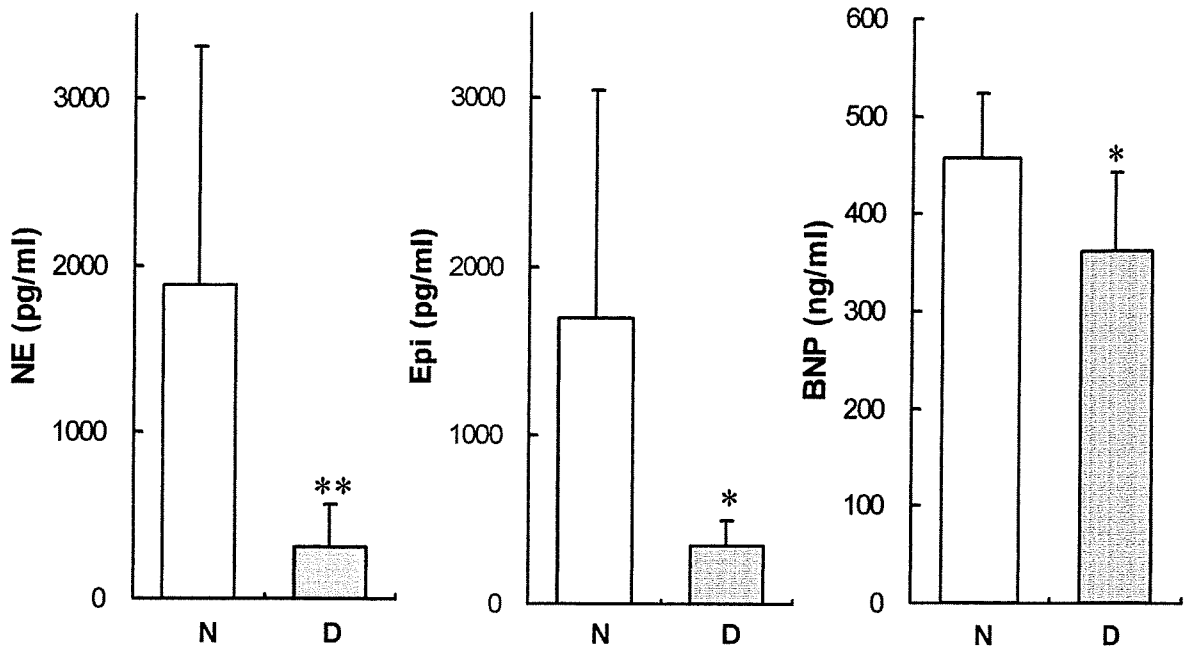


Blood concentrations of norepinephrine (NE), epinephrine (Epi) and brain natriuretic protein (BNP) at week 6 of treatment. Significant decreases in blood NE, Epi and BNP concentrations were observed in the donepezil group (shaded bar, D) compared to the nontreated group (open bar, N). *: $p<0.05$, **: $p<0.01$

**Figure 4.**

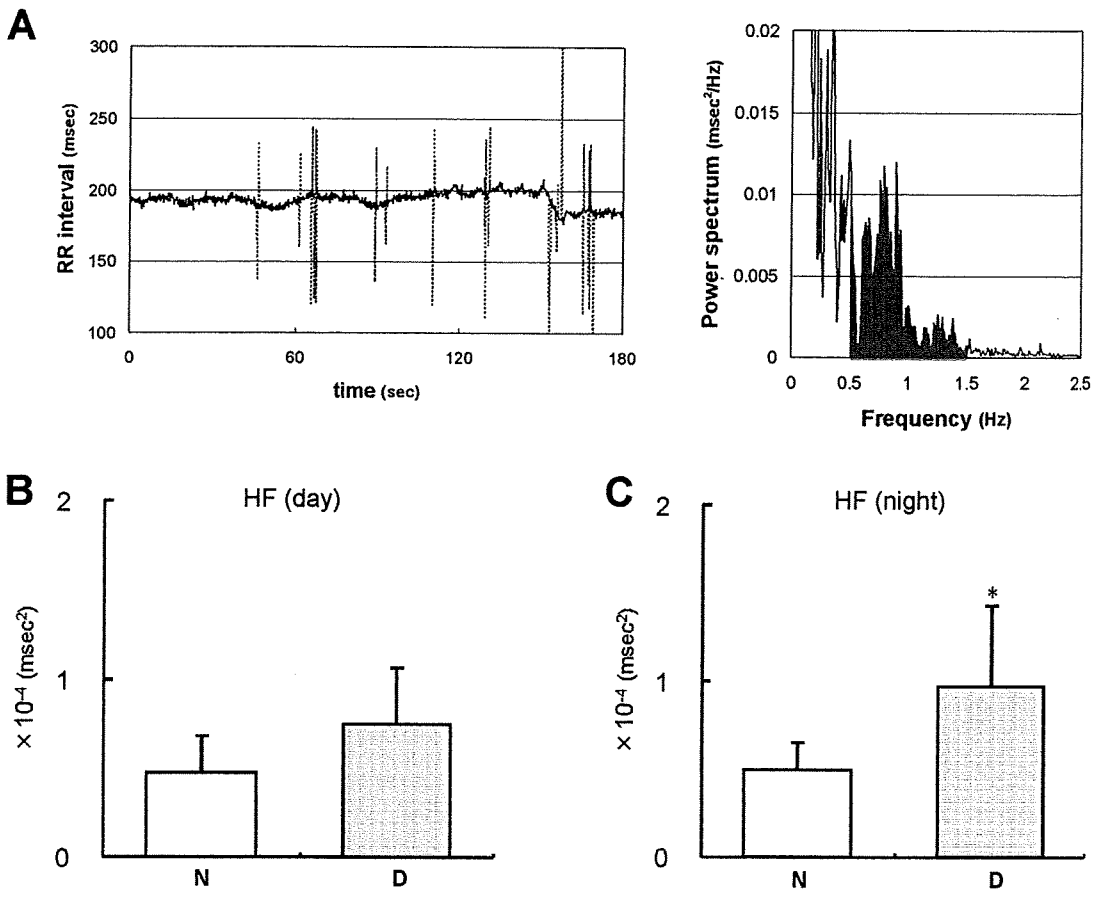


**A:** A representative example of time series of RR interval (left) and its power spectrum (right) in a donepezil-treated rat. RR intervals shown with dotted lines were judged as extrasystoles or post-extrasystoles and were removed before calculating power spectrum. Solid area indicates high frequency component (HF). **B:** HF of heart rate variability during the day. No significant difference in daytime HF value was observed between the donepezil group (shaded bar, D) and the nontreated group (open bar, N). **C:** High frequency component (HF) of heart rate variability during the night. A significant increase in nocturnal HF value was observed in the donepezil group (shaded bar, D) compared to the nontreated group (open bar, N). *: $p<0.05$ by t-test using log(HF) values

J Artif Organs (2009) 12:111–117
DOI 10.1007/s10047-009-0449-4



ORIGINAL ARTICLE

Azizi Miskon, MEng · Tomo Ehashi, PhD
Atsushi Mahara, PhD · Hiroshi Uyama, PhD
Tetsuji Yamaoka, PhD

# Beating behavior of primary neonatal cardiomyocytes and cardiac-differentiated P19.CL6 cells on different extracellular matrix components

**Abstract** Stem cell-based therapy in cardiac tissue engineering is an emerging field that shows great potential for treating heart diseases. However, even preliminary issues, such as the ideal niche for cardiomyocytes, have not been clarified yet. In the present study, the effects of extracellular matrix (ECM) components on the beating duration of neonatal rat cardiomyocytes (RCMs) and on the cardiac differentiation of P19.CL6 carcinoma stem cells were studied. RCMs were cultured on gelatin-, fibronectin-, and collagen type I-coated dishes and on noncoated polystyrene dishes, and their beating rate, beating duration, and cardiac gene expression were evaluated. The beating period and the expression of troponin T type-2 (TNNT2) and troponin C type-1 (TNNC1) of cardiomyocytes cultured on gelatin-coated dishes were longer and higher than for those on dishes with other coatings. For the cardiac differentiation of P19.CL6 cells, troponin T type-2 expression on gelatin- and fibronectin-coated dishes was five times that on collagen type I-coated dishes or polystyrene dishes 11days after induction. These results indicate that a gelatin-coated surface has a high ability not only to maintain the cardiac phenotype but also to enhance cardiac differentiation.

**Key words** Extracellular matrix · Cardiomyocyte · Beating · Differentiation

Received: September 5, 2008 / Accepted: January 14, 2009

A. Miskon · T. Ehashi · A. Mahara · T. Yamaoka (✉)
Department of Biomedical Engineering, Advanced Medical Engineering Center, National Cardiovascular Center Research Institute, 5-7-1 Fujishiro-dai, Suita, Osaka 565-8565, Japan
Tel. +81-6-6833-5012 ext. 2637; Fax +81-6-6835-5476
e-mail: yamtet@ri.ncvc.go.jp

A. Miskon · H. Uyama
Department of Chemical Engineering, Osaka University, Osaka, Japan

## Introduction

Cardiac tissue engineering, such as cardiomyocyte transplantation for patients with ischemic heart disease or dilated cardiomyopathies, is of great potential therapeutic value to enhance the contractile function of the failing heart. Recently, fetal or neonatal rat cardiomyocytes were reported to form mature cardiac tissue in syngeneic hearts, acutely injured myocardium, and granulation tissue in the heart.[1] However, the best cell sources for clinical cardiomyocyte transplantation are still under debate. In general, three types of potential cell sources have been proposed.[2] One is the allogeneic source, including human embryonic stem cells or fetal allogeneic cardiomyocytes, but there still remain ethical issues. Another is the transgenic source. Genetically engineered animal cardiomyocytes have been studied in an attempt to reduce the rejection reaction in vivo, which is still a long-term problem in recipients.

The most promising cell source is the autogeneic one. Isolating cardiomyocytes from patients' hearts is unrealistic at present, and autologous skeletal muscle precursors, fibroblasts, or mesenchymal stem cells have been studied so far.[3] However, since beating cardiomyocytes are more promising,[4] we have been trying to differentiate bone marrow mesenchymal stem cells (BMSCs) into "beating" cardiomyocytes. There is no certain induction method for BMSC differentiation into beating cardiomyocytes. Many researchers have observed cardiac gene expression in MSCs treated with various inducers[5–7] or passage numbers,[8] but they do not beat spontaneously. Wakitani et al. and Makino et al. reported that murine BMSCs were differentiated to beating cardiomyocyte-like cells in vitro by exposing them to DNA-demethylating agent 5-azacytidine.[5,6] This is in contrast with a report stating that functional cardiac cells and gene expression were not obtained by treatment with 5-azacytidine.[9]

Producing autologous beating cardiomyocytes is thus an attractive goal for cell-based therapy. The crucial part is how to differentiate cells to cardiomyocytes in vitro and how to maintain the beating. Various microenvironments surrounding the cells (niches) play important roles not only

in cell proliferation but also in cell differentiation. The effect of extracellular matrix (ECM) proteins such as collagen type I, collagen type IV, gelatin, laminin, fibronectin, Matrigel (a mixture of laminin, collagen type IV, heparan sulfate proteoglycans, and entactin), and Cardiogel (a mixture of collagen types I and III, glycoproteins, laminin, fibronectin, and proteoglycans) on cell viability, proliferation rate, and cardiomyocyte gene expression have been reported;[10,11] however, the cardiomyocyte beating behavior has not fully been discussed.

In the present study, differentiation to beating cardiomyocytes and the beating duration of the cardiomyocytes were studied using two types of model cells. Murine embryonal carcinoma (EC) stem cells (P19.CL6),[12] which are widely used for investigating cardiac differentiation, were treated with differentiation medium containing 1% dimethyl sulfoxide (DMSO) on various ECM proteins (collagen, type I gelatin, and fibronectin), and their differentiation efficiency was evaluated. The effect of these substrates on the beating duration of rat neonatal cardiomyocytes was also investigated, along with intracellular cardiac marker genes [troponin T type-2 (TNNT2) and troponin C type-1 (TNNC1)][13] and skeletal muscle marker gene [troponin C type-2 (TNNC2)], which is reported to be expressed in the early developing heart.[14] Any fundamental information obtained would be important for the cardiac differentiation of various stem cells, including autologous BMSCs.

## Materials and methods

### Cardiomyocytes

Cardiomyocytes were isolated from neonatal Sprague–Dawley rat heart (1 to 2 days old) by the collagenase digestion method with modifications.[15,16] Institutional guidelines for the care and use of laboratory animals were observed. The hearts were removed and carefully minced with a scalpel blade into fragments and were rinsed several times with Hanks' balanced salt solution (Sigma-Aldrich, St. Louis, MO, USA) to remove blood and cellular debris. The minced hearts were gently stirred in 50 ml collagenase solution [0.15 M Sodium Chloride (NaCl), 5.63 mM Potassium Chloride (KCl), 0.02 M 4-(2-hydroxyethyl)-1-piperazineethanesulfonic acid (HEPES), 0.02 M Sodium Hydrogen Carbonate ($NaHCO_3$), 3.74 mM Calcium Chloride Dihydrate ($CaCl_2{\cdot}2H_2O$), and $6.5 \times 10^4$ U collagenase (Wako, Osaka, Japan, Lot no: 06032W)] at 37°C for 30 min. The resulting cell suspension was filtered through a nylon cell strainer (BD Falcon, BD Biosciences, Bedford, MA, USA) with a 40-μm pore size and centrifuged at 78 g for 3 min.

Isolated cardiomyocytes ($1.0 \times 10^5$) were cultured in minimum essential medium alpha medium (α-MEM, Gibco, Invitrogen, Grand Island, NY, USA) supplemented with 10% (v/v) fetal bovine serum (FBS, MP Biomedicals, Eschwege, Germany, lot no: 7297H), and 100 IU/l penicillin–streptomycin (Wako, Osaka, Japan) on 60-mm gelatin-(IWAKI, Asahi Glass, Tokyo, Japan), fibronectin-(BD Falcon, BD BioCoat, BD Biosciences), or collagen type I-coated dishes and noncoated polystyrene dishes (IWAKI).

### Differentiation of P19.CL6 cells

Differentiation of P19.CL6 cells was performed as described by Ohkubo with modifications.[12] Briefly, P19.CL6 cells were plated at a density of $3.7 \times 10^5$ cells on 60-mm gelatin-, fibronectin-, or collagen type I-coated dishes or noncoated polystyrene dishes with a α-MEM supplemented with 10% (v/v) FBS containing 1% DMSO (Wako). As a control experiment, P19.CL6 cells were cultured with α-MEM supplemented with 10% (v/v) FBS without 1% DMSO. The medium was changed every 2 days.

### Measurement of action potential

Cultured plates on which beating colonies appeared were placed on the stage of an inverted phase-contrast optical microscope (ZEISS, Axiovert 135, Munich, Germany) and action potentials were measured immediately by a conventional microelectrode. The measurements were conducted after 1, 2, and 3 weeks of cultivation. Silicon-coated Ag wire (A-M System, Carlsborg, WA, USA, 250 μm bare, 330 μm coated) was used as the microelectrode. The microelectrode was set in a micromanipulator system (MON-202D, Nikon Narishige, Tokyo, Japan) and connected to a bioelectric amplifier (AB-621G, Nihon Kohde, Osaka, Japan). The sensitivity and time constant of the bioelectric amplifier were set at 0.1 mV/div and 0.003 s. For the measurements, the microelectrode was adjusted using the micromanipulator until it was attached to the membrane of beating cells. The voltage difference was amplified by the bioelectric amplifier and was displayed and recorded using Chart 5 software (AD Instrument, Bella Vista, Australia).

### Total RNA isolation and reverse transcription

Total RNAs of cardiomyocytes and DMSO-treated P19.CL6 cells cultured on various dishes were extracted by QuickGene RNA cultured cell kit S (Fujifilm Life Science, Tokyo, Japan) 4 weeks after culture and 11 days after culture, respectively.

First-strand cDNAs were synthesized using a mixture of oligo$(dT)_{18}$ primer. Total cellular RNAs (200 ng) were incubated with 2.5 μM oligo$(dT)_{18}$ primer at 70°C for 10 min to denature the RNA secondary structure and then incubated at 4°C to let the primer anneal to the RNA. A given amount of 5X RT buffer (Toyobo, Osaka, Japan) and 2.5 mM Deoxynucleotide Trisphasphate (dNTP) mixture (Takara Bio, Shiga, Japan) (4 μl) were added and incubated at 37°C for 5 min. The reverse transcriptase (100 Units, Toyobo) was added into the mixture and the reverse transcriptase (RT) reaction was extended at 37°C for 1 h. Then, the reac-

**Table 1.** Polymerase chain reaction primers used in this study

| Genes | Sense | Antisense |
|---|---|---|
| TNNT2 | 5′-GAAACAGGATCAACGACAACCA-3′ | 5′-CGCCCGGTGACTTTGG-3′ |
| TNNC1 | 5′-GATCTCTTCCGCATGTTTGACA-3′ | 5′-TGGCCTGCAGCATCATCTT-3′ |
| TNNC2 | 5′-AGATCGAATCCCTGATGAAGGA-3′ | 5′-CATCTTCAGAAACTCGTCGAAGTC-3′ |
| GAPDH | 5′-CTACCCCCAATGTATCCGTTGT-3′ | 5′-TAGCCCAGGATGCCCTTTAGT-3′ |

GAPDH, Glyceraldehyde 3 phosphate dehydrogenase

**Table 2.** Summary of voltage potentials for cardiomyocytes cultured in several types of extracellular matrix-coated dishes

| Substrate | Action potential (mV) [Beating rate (Hz)] | | |
|---|---|---|---|
| | Day 7 | Day 14 | Day 21 |
| Gelatin | 6.7 ± 0.49 [1.2 ± 0.05] | 6.6 ± 1.26 [1.3 ± 0.01] | 3.1 ± 0.21[2.8 ± 0.03] |
| Fibronectin | 1.1 ± 0.97 [1.1 ± 0.30] | 6.9 ± 1.15 [1.3 ± 0.42] | 2.8 ± 0.11[2.0 ± 0.11] |
| Collagen type-I | 2.6 ± 0.35 [0.8 ± 0.02] | 1.7 ± 0.03 [2.3 ± 0.05] | ND |
| Polystyrene | 2.0 ± 0.75 [0.3 ± 0.04] | ND | ND |

ND, not done

tion mixture was heated at 94°C for 5 min to inactivate the enzyme and cooled at 4°C for 15 min. The RNase (DNase-free, 0.5 μg, Roche Diagnostics, Mannheim, Germany) was added to the mixture and incubated at 37°C to remove the template of RNA.

### Real-time quantitative polymerase chain reaction

Real-time quantitative polymerase chain reaction (PCR) was conducted with SYBR Green. Primers for PCR analysis for troponin T type-2, troponin C type-1, and troponin C type-2 were designed using Primer Express software (Perkin-Elmer Applied Biosystems, Warrington, UK). The primer sequences are shown in Table 1. The reaction mixtures contained 23.74 μl distilled water, 25 μl SYBR Green Realtime PCR master mix (Toyobo), 100 nM of each primer, and 0.26 μl cDNA. The thermal profile for PCR was 50°C for 2 min, followed by 95°C for 10 min, followed by 40 cycles of 15 s at 95°C and 1 min at 60°C. Distilled water 0.26 μl was used as a negative control PCR reaction to ensure the absence of template contamination in PCR reagents. The average threshold cycle (Ct) values of triplicate measurements were used for all subsequent calculations on the basis of the delta Ct method.

## Results

### Beating behavior of isolated cardiomyocytes

One week after culture, the action potential of cardiomyocytes on gelatin-coated dishes was higher than that for other conditions (Fig. 1), and the beating duration was also longer than that for other conditions. The action potential and beating rates on each matrix are summarized in Table 2. After 7 days of culture, the action potential was around 6.7 ± 0.49 mV for cardiomyocytes cultured on gelatin-coated dishes, 1.1 ± 0.97 mV on fibronectin-coated dishes, 2.0 ± 0.35 mV on collagen type I-coated dishes, and 2.0 ± 0.75 mV on noncoated polystyrene dishes. These results indicate that the beating rate on fibronectin-coated dishes, collagen type I-coated dishes, and noncoated polystyrene dishes were 84%, 61%, and 70% lower than the beating rate on gelatin-coated dishes after 1 week of cultivation.

After 14 days of culture, the action potential became 6.6 ± 1.26 mV on gelatin-coated dishes, 6.9 ± 1.15 mV on fibronectin-coated dishes, and 1.7 ± 0.03 mV on collagen type I-coated dishes. No beating was observed on noncoated polystyrene dishes after 2 weeks of cultivation. After 21 days of culture, the action potential was 3.1 ± 0.21 mV on gelatin-coated and 2.8 ± 0.11 mV on fibronectin-coated dishes. No action potential was detected on collagen type I-coated dishes and polystyrene dishes.

The beating rate of cardiomyocytes was also affected by the ECM proteins. After 7 days of culture, the beating rate of cardiomyocytes was 1.2 ± 0.05 Hz on gelatin-coated dishes, 1.1 ± 0.3 Hz on fibronectin-coated dishes, 0.8 ± 0.02 Hz on collagen type I-coated dishes, and 0.3 ± 0.04 Hz on noncoated polystyrene dishes. After 14 days of culture, the beating rate became 1.3 ± 0.01 Hz on gelatin-coated dishes, 1.3 ± 0.42 Hz on fibronectin-coated dishes, and 2.3 ± 0.05 Hz on collagen type I-coated dishes. After 21 days, the beating rate was 2.8 ± 0.03 Hz on gelatin-coated dishes and 2.0 ± 0.11 Hz on fibronectin-coated dishes, whereas cardiomyocytes cultured on noncoated polystyrene dishes and collagen-coated dishes did not beat well and stopped at an early stage of cultivation. These results indicate that gelatin could maintain the beating behavior of cardiomyocytes for a longer time compared to fibronectin or collagen type I.

### Expression of troponin T type-2 and troponin C type-1

Cardiac troponin T type-2 and troponin C type-1 are known to be cardiomyocyte markers and are important in the structure of muscle tissue; they also play a role in the contraction of muscle cells.[13] After 4 weeks of culture,

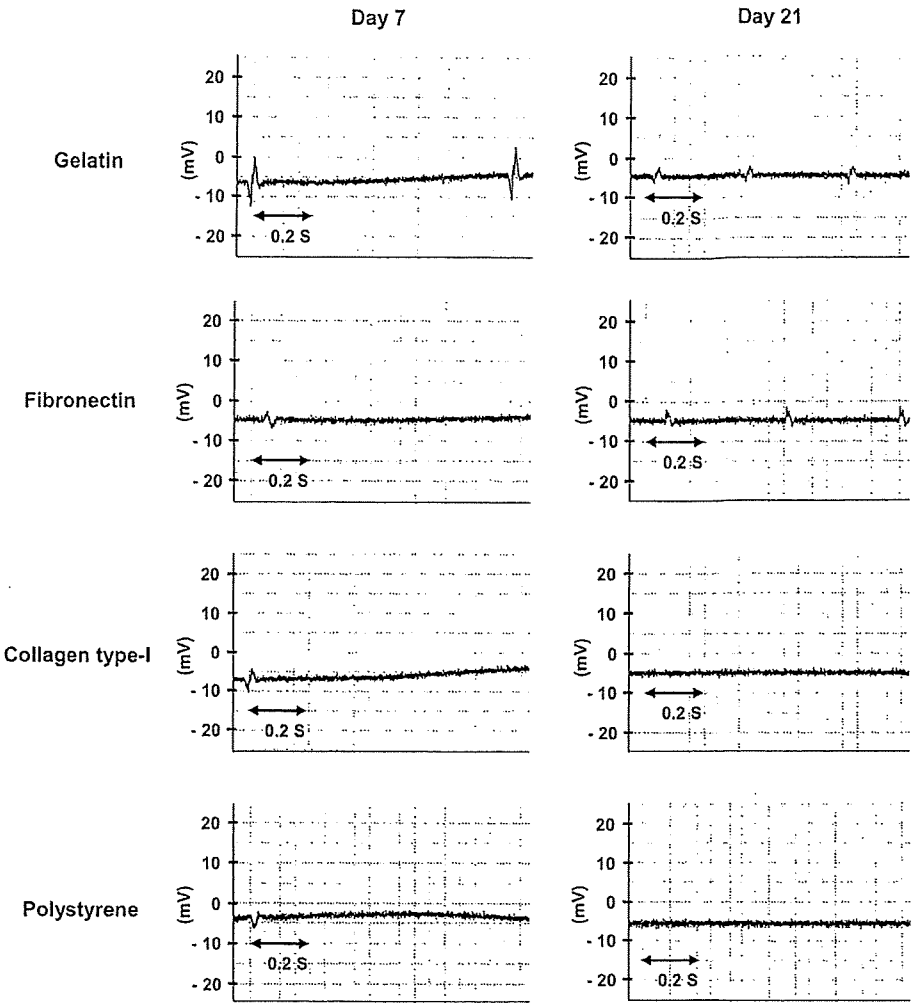


**Fig. 1.** Electrophysiological assessment of isolated cardiomyocytes after 7 and 21 days of cultivation on different substrates

expression of troponin T type-2 in cardiomyocytes on gelatin-coated dishes was 7, 6, and 12 times higher than those on fibronectin-coated, collagen-coated, and non-coated dishes (Fig. 2A). Expression of troponin C type-1 on gelatin-coated dishes was also 5, 6, and 32 times higher than those on fibronectin-coated, collagen type I-coated, and noncoated dishes (Fig. 2B). These results are consistent with the results of the electrophysiological study (Fig. 1), in which the beating of cardiomyocytes still could be detected on gelatin- and fibronectin-coated dishes after 3 weeks of cultivation.

## Differentiation of P19.CL6 cells

Beating colonies were found on gelatin-coated dishes in 9 days with α-MEM medium containing 1% DMSO. This was followed by cells cultured on fibronectin-coated dishes after 10 days of culture and collagen type I-coated dishes after 11 days of culture. The average number of beating colonies found on the first day of detection was 13 ± 7 colonies per dish on gelatin-coated dishes, 9 ± 5 colonies per dish on fibronectin-coated dishes, 5 ± 2 colonies on collagen type I-coated dishes, and 3 ± 1 colonies on polystyrene dishes (Table 3).

As described earlier, troponin T type-2 and troponin C type-1 are known to be markers of cardiomyocytes,[13] and troponin C type-2 is reported to be a marker of cardiac development.[14] Expression of troponin T type 2 on gelatin- and fibronectin-coated dishes was higher than that for the other dishes, as shown in Fig. 3A. However, the expression of troponin C type-2 in collagen type I-coated dishes and noncoated polystyrene dishes was higher than that in gelatin- and fibronectin-coated dishes. The high expression of troponin C type-2 on collagen type I coated dishes and noncoated polystyrene dishes on day 11 was possibly because of the delayed differentiation of P19.CL6 cells to cardiomyocytes-like cells. Stoutamyer and Dhoot reported that troponin C type-2 was first expressed on day 3, reached maximum expression on day 5, and decreased day by day until no expression was found on day 11 during the development of quail heart in ovo.[14] Stoutamyer and Dhoot also reported that the expression of troponin C type-1 was detected on day 2 and decreased during the increase of

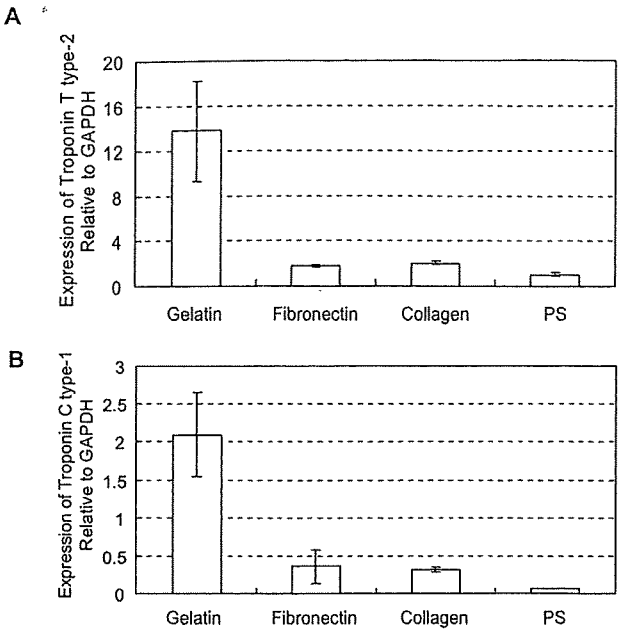


**Fig. 2.** Expression of cardiac markers (**A** troponin T type-2 and **B** troponin C type-1) in isolated cardiomyocytes after cultivation for 4 weeks on various types of extracellular matrix. *GAPDH*, Glyceraldehyde 3 phosphate dehydrogenase; *PS*, polystyrene

**Table 3.** Number of beating colonies of P19.CL6 cells 11 days after induction with 1% dimethyl sulfoxide

| Substrate | Average number of beating colonies per dish |
|---|---|
| Gelatin | 13 ± 7 |
| Fibronectin | 9 ± 5 |
| Collagen type-I | 5 ± 2 |
| Polystyrene | 3 ± 1 |

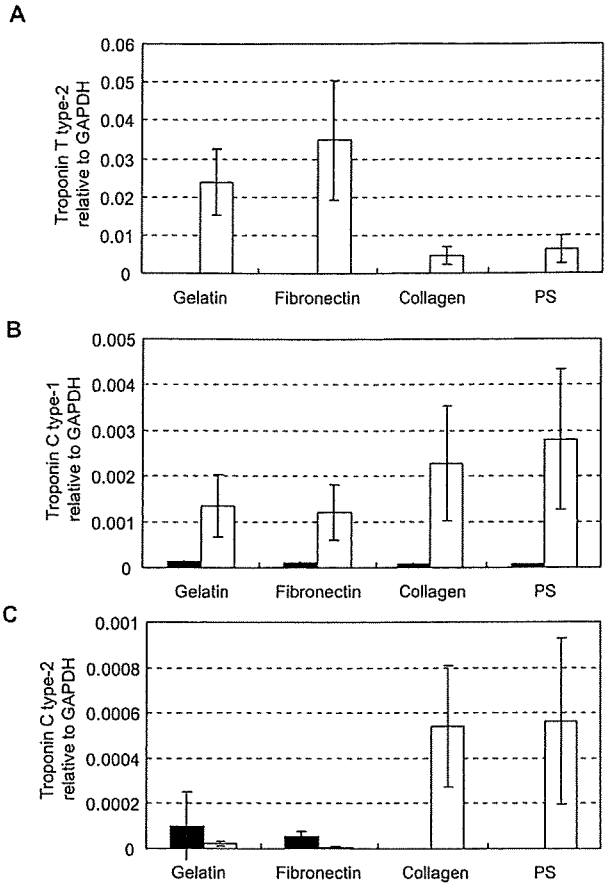


**Fig. 3.** Expression of cardiac markers in P19.CL6 cells (**A** troponin T type-2, **B** troponin C type-1, **C** troponin C type-2) treated with minimum essential medium alpha medium (α-MEM) containing 1% dimethyl sulfoxide on various dishes (*white bars*) or with α-MEM as a control for 11 days (*black bars*) PS, polysyrene

troponin C type-2, reaching a constant level after that.[14] In addition, the troponin C type-2 expression on a collagen-coated or noncoated dish may suggest skeletal muscle differentiation of P19.CL6 cells, although further analysis is needed.

These results demonstrated that differentiation of P19.CL6 cells to beating cells on gelatin-coated dishes and fibronectin-coated dishes was faster and more effective than that on collagen type I-coated dishes and noncoated polystyrene dishes.

## Discussion

In the present study, enhanced action potentials and elongated beating durations of neonatal cardiomyocyte were observed on gelatin-coated dishes compared to those on collagen type I-coated dishes. Possible differences between gelatin and collagen are: (1) collagen posses a triple-helical conformation, (2) gelatin has a wide molecular weight distribution depending on its preparation process, (3) gelatin is easily hydrolyzed by protease,[17] (4) the dynamic storage modulus of gelatin is higher than that of collagen,[18] and (5) gelatin binds with fibronectin with a higher affinity.[19–21] It has already been reported that fibronectin is a very elastic substrate.[22]

The mechanism of the elongated beating duration on gelatin-coated substrate is unclear, but the mechanical properties (elasticity) and biological activity of the substrates might be influential. It has been reported that the mechanical properties of culture matrices affect various cellular properties such as the morphology of embryonic stem cells,[23,24] the collagen production of fibroblasts,[25,26] and the differentiation of mesenchymal and neural stem cells.[27,28]

Fibronectin produced by culture cells is known to associate with the fibronectin-binding domain of collagen, resulting in fibrillogenesis.[21] It has also been reported that fibronectin binds to gelatin more strongly than to collagen.[20,21] Therefore, the high production of fibrils might occur more effectively on gelatin-coated dishes than on fibronectin- or collagen-coated dishes. These connecting elastic fibers might regulate the motion of cardiomyocytes during

contraction and recoil, as suggested by Ahumada and Saffitz.[29] The highly elastic features of matrices made of gelatin, fibronectin bound onto gelatin,[18,22] and developed fibrin matrices may allow easier contraction of cardiomyocytes, leading to larger action potentials and longer beating durations on gelatin.

P19.CL6 cells were used to study the effect of culture substrates on cardiogenesis in vitro because Ohkubo reported that P19.CL6 cells differentiated into cardiomyocytes in 10 days after DMSO treatment, and observation of differentiation continued for 11 days. The first beating colony was found on the 9th day on gelatin-coated dishes, on the 10th day on fibronectin-coated dishes, and on the 11th day on collagen type I-coated dishes and noncoated polystyrene dishes. The expressions of troponin T type-2 on gelatin- and fibronectin-coated dishes were significantly higher than those on collagen type I-coated dishes and on noncoated polystyrene dishes. High expression of troponin C type-2 in collagen type I-coated dishes and noncoated polystyrene dishes is considered to indicate delayed cardiac differentiation or skeletal muscle differentiation of P19. CL6.

The differentiation of P19.CL6 cells on gelatin- and collagen type I-coated dishes was very different, despite their similar unit structure. The fast differentiation on gelatin was possibly because of slow cell proliferation on high-dynamic-storage-modulus substrates.[18] The growth of P19.CL6 cells on gelatin-coated dishes was about half that on collagen type I-coated dishes (data not shown). Walsh et al. suggested that the proliferation of mesenchymal stem cells was suppressed during the differentiation to osteoblasts in vitro.[30] The fast differentiation on fibronectin-coated dishes may also relate to the elasticity of the substrate.[22]

This finding will hopefully offer a bright future for the myocardial patch scaffold. It has been reported that the probability of cardiac differentiation of adipose tissue-derived mesenchymal stem cells after transplantation to infracted rat heart is quite low.[31] In the present study, the gelatin-based niche was found to be preferable for cardiac differentiation and for the beating function of cardiomyocytes. We will be applying these results to the cardiac differentiation of mesenchymal stem cells in order to prepare allogeneic beating cardiomyocytes.

## Conclusion

The physical and biological properties of the substrate were the important factors not only for maintaining cardiac functions but also for leading to the cardiac differentiation of P19.CL cells. Gelatin was found to be a promising ECM protein to this end in vitro.

**Acknowledgments** This work was partly supported by a Grant-in-Aid for Scientific Research (B) from the Ministry of Education, Culture, Sports, Science and Technology of Japan. The author (Azizi Miskon) would like to thank the Ministry of Higher Education, Malaysia, and Tun Hussein Onn of the University of Malaysia for funding his study under the Academic Training Scheme.

## References

1. Li RK, Mickle DA, Weisel RD, Zhang J, Mohabeer MK. In vivo survival and function of transplanted rat cardiomyocytes. Circ Res 1996;78:283–288
2. El Oakley RM, Ooi OC, Bongso A, Yacoub MH. Myocyte transplantation for myocardial repair: a few good cells can mend a broken heart. Ann Thorac Surg 2001;71:1724–1733
3. Ott HC, Davis BH, Taylor DA. Cell therapy for heart failure – muscle, bone marrow, blood, and cardiac-derived stem cells. Semin Thorac Cardiovasc Surg 2005;17:348–360
4. Segers VF, Lee RT. Stem-cell therapy for cardiac disease. Nature 2008;451:937–942
5. Makino S, Fukuda K, Miyoshi S, Konishi F, Kodama H, Pan J, Sano M, Takahashi T, Hori S, Abe H, Hata J, Umezawa A, Ogawa S. Cardiomyocytes can be generated from marrow stromal cells in vitro. J Clin Invest 1999;103:697–705
6. Wakitani S, Saito T, Caplan AI. Myogenic cells derived from rat bone marrow mesenchymal stem cells exposed to 5-azacytidine. Muscle Nerve 1995;18:1417–1426
7. Xu W, ZhangX, Qian H, Zhu W, Sun X, Hu J, Zhou H, Chen Y. Mesenchymal stem cells from adult human bone marrow differentiate into a cardiomyocyte phenotype in vitro. Exp Biol Med 2004; 229:623–631
8. Zhang FB, Li L, Fang B, Zhu DL, Yang HT, Gao PJ. Passage-restricted differentiation potential of mesenchymal stem cells into cardiomyocyte-like cells. BBRC 2005;336:784–792
9. Liu Y, Song J, Liu W, Wan Y, Chen X, Hu C. Growth and differentiation of rat bone marrow stromal cells: does 5-azacytidine trigger their cardiomyogenic differentiation? Cardiovasc Res 2003;58:460–468
10. Macfelda K, Kapeller B, Wilbacher I, Losert UM. Behavior of cardiomyocytes and skeletal muscle cells on different extracellular matrix components – relevance for cardiac tissue engineering. Artif Organs 2007;31:4–12
11. Bird SD, Doevendans PA, van Rooijen MA, Brutel de la Riviere A, Hassink RJ, Passier R, Mummery CL. The human adult cardiomyocyte phenotype. Cardiovasc Res 2003;58:423–434
12. Ohkubo AH. Differentiation of beating cardiac muscle cells from a derivative of P19 embryonal carcinoma cells. Cell Struct Funct 1996;21:101–110
13. Saggin L, Ausoni S, Gorza L, Sartore S, Schiaffino S. Troponin T switching in the developing rat heart. J Biol Chem 1998;263: 18488–18492
14. Stoutamyer A, Dhoot GK. Transient expression of fast troponin C transcripts in embryonic quail heart. J Muscle Res Cell Motil 2005;26:237–245
15. Seglen PO. Preparation of isolated rat liver cells. Methods Cell Biol 1976;13:29–83
16. Moldeus P, Högberg J, Orrenius S. Isolation and use of liver cells. Methods Enzymol 1978;52:60–71
17. Zhang Z, Li G, Shi B. Physicochemical properties of collagen, gelatin, and collagen hydrolysate derived from bovine limed split wastes. J Soc Leather Technol Chem 2006;90:23–28
18. Chien JC, Chang EP. Dynamic mechanical and rheo-optical studies of collagen and gelatin. Biopolymers 1972;11:2015–2031
19. Little CD, Chen WT. Masking of extracellular collagen and the co-distribution of collagen and fibronectin during matrix formation by cultured embryonic fibroblast. J Cell Sci 1982;55: 35–50
20. Engvall E, Ruoslahti E, Miller ED. Affinity of fibronectin to collagens of different genetic types and to fibrinogen. J Exp Med 1978;147:1584–1595
21. Dzamba BJ, Wu H, Jaenisch R, Peters DM. Fibronectin binding site in type I collagen regulates fibronectin fibril formation. J Cell Biol 1993;121:1165–1172
22. Erickson HP. Stretching fibronectin. J Muscle Res Cell Motil 2002;23:575–580
23. Bard JB, Hay ED. The behavior of fibroblasts from the developing avian cornea. Morphology and movement in situ and in vitro. J Cell Biol 1975;67:400–418
24. Hay ED. Interaction of embryonic surface and cytoskeleton with extracellular matrix. Am J Anat 1982;165:1–12

25. Nakagawa S, Pawelek P, Grinnell F. Extracellular matrix organization modulates fibroblast growth and growth factor responsiveness. Exp Cell Res 1989;182:572–582
26. Halliday NL, Tomasek JJ. Mechanical properties of the extracellular matrix influence fibronectin fibril assembly in vitro. Exp Cell Res 1995;217:109–117
27. Engler AJ, Sen S, Sweeney HL, Discher DE. Matrix elasticity directs stem cell lineage specification. Cell 2006;126:677–689
28. Saha K, Keung AJ, Irwin EF, Li Y, Little L, Schaffer DV, Healy KE. Substrate modulus directs neural stem cell behavior. Biophys J 2008;95:4426–4438
29. Ahumada GG, Saffitz JE. Fibronectin in rat heart: a link between cardiac myocytes and collagen. J Histochem Cyotchem 1984;4: 383–388
30. Walsh S, Jordan GR, Jefferiss C, Stewart K, Beresford JN. High concentrations of dexamethasone suppress the proliferation but not the differentiation or further maturation of human osteoblast precursors in vitro: relevance to glucocorticoid-induced osteoporosis. Rheumatology 2001;40:74–83
31. Miyahara Y, Nagaya N, Kataoka M, Yanagawa B, Tanaka K, Hao H, Ishino K, Ishida H, Shimizu T, Kangawa K, Sano S, Okano T, Kitamura S, Mori H. Monolayered mesenchymal stem cells repair scarred myocardium after myocardial infarction. Nat Med 2006;12: 459–465

Polymer Degradation and Stability 94 (2009) 1349–1353

Contents lists available at ScienceDirect

Polymer Degradation and Stability

journal homepage: www.elsevier.com/locate/polydegstab

# Self-assemblies of enzymatically degradable amphiphilic oligopeptides as nonviral gene carrier

Tomoko Hashimoto [a,b], Reiko Iwase [b,c], Akira Murakami [b], Tetsuji Yamaoka [a,b,*]

[a] Department of Biomedical Engineering, National Cardiovascular Center Research Institute, 5-7-1 Fujishirodai, Suita, Osaka 565-8565, Japan
[b] Department of Biomolecular Engineering, Kyoto Institute of Technology, Matsugasaki, Sakyo-ku, Kyoto 606-8585, Japan
[c] Department of Biosciences, Teikyo University of Science and Technology, 2525 Yatsusawa, Uenohara, Yamanashi 409-0193, Japan

ARTICLE INFO

*Article history:*
Received 25 April 2009
Received in revised form
25 May 2009
Accepted 28 May 2009
Available online 6 June 2009

*Keywords:*
Polymeric gene carrier
Self-assembly
Stability
Oligopeptide
Molecular weight

ABSTRACT

Novel biodegradable oligopeptide-type gene carriers composed of cationic residues (KRRRKRKRRRKRKRRC) and oligo leucine segments were developed. The amphiphilic carrier was found to form micelle-like assemblies in aqueous solutions, when the oligo leucine is 12 amino acids length (Pep-L12). NMR, CMC, and GPC analysis revealed their hydrophobic/cationic core/shell morphology. Hydrophobic interaction between leucines is thought to be the major driving force behind formations of assemblies. The transient expression of luciferase introduced to COS-1 cells using Pep-L12 below the CMC is as low as that by the control cationic peptides without leucine residue (Pep-L0), while improved transgene expression was observed in the case of Pep-L12 above CMC. The self-assembly raised the apparent molecular weight and gene transfection ability without loosening their low cytotoxicity. These results indicate that the amphiphilic oligopeptides are very promising materials as highly efficient and less toxic gene carriers.



## 1. Introduction

Polymeric gene carriers are now extensively studied due to their high abilities to deliver and protect pDNA, but the polyplexes formed between the carriers and pDNAs are sometimes too highly compacted to be recognized by transcription factors in nucleus. Recently, the destabilization of the polyplexes by conjugating hydrophilic or hydrophobic segments to polymeric carriers has been reported [1–3]. However, excess modification of side chains results in the low resistance to DNase at the same time.

Effect of the carrier molecular weights (Mws) has been also being studied [4–8]. Recently, high potential of low Mw polymeric carriers was attracting great attention. Kunath et al. reported that low Mw PEI (5 kDa) was much less toxic than high Mw PEI (48 kDa), and reporter gene expression of 5 kDa PEI was 3.7-fold higher than 48 kDa PEI in various cell lines [6]. Breuning et al. compared PEIs with the Mw of 1–9 kDa and showed that the highest reporter gene expression was obtained at 5.6 kDa, with low cytotoxicity. Schaffer et al. reported higher gene expression for low Mw PLL (19 and 36 residues) than high Mw PLL (180 residues) because of effective *in vitro* transcription and easy pDNA release [4]. Taken together, low cytotoxicity and high DNA releasing ability of low Mw carries were important key features for the high potential gene carriers. On the other hand, low Mw carriers are pointed out to reduce cellular uptake [9] and decrease stability of polyplexes at the same time. Thus, a new type "low Mw carriers", which have low cytotoxicity, high cellular uptake, and adequate polyplex stability, would be more useful gene carriers.

In the present study, oligopeptide-type carriers were selected in order to reduce cytotoxicity and to induce the intracellularly digestible feature. Since the chemical chain elongation of cationic oligopeptide would increase the cytotoxicity, we tried to raise the apparent Mw of oligopeptide-type carriers by their self-assembly. Amphiphilic oligopeptides having cationic and hydrophobic sequences were then designed. Hydrophobic interactions between oligo leucine sequences make carriers form assemblies and increase the apparent Mw. Cationic sequences for interacting with pDNA include cleavable sequences (Arg-X-Lys/Arg-Arg (R-X-K/R-R)) by intracellular proprotein convertase, furin [10,11]. We have previously found that carriers including this cleavable sequences are enough cationic to form polyplexes with pDNA, and these polyplexes became destabilized if carriers were cleaved by furin [12]. Increased apparent Mw is expected to increase cellular uptake of the polyplex and the enhanced stability can be destabilized by furin cleavage resulting in the pDNA release in intracellular environments.

* Corresponding author at: Department of Biomedical Engineering, National Cardiovascular Center Research Institute, 5-7-1 Fujishirodai, Suita, Osaka 565-8565, Japan. Tel.: +81 6 6833 5012x2637; fax: +81 6 6835 5476.
*E-mail address:* yamtet@ri.ncvc.go.jp (T. Yamaoka).

0141-3910/$ – see front matter © 2009 Elsevier Ltd. All rights reserved.
doi:10.1016/j.polymdegradstab.2009.05.021

## 2. Experimental

### 2.1. Amphiphilic oligopeptides

We synthesized four oligopeptides by Fmoc-based solid phase method using 9050 plus PepSynthesizer (Applied Biosystems, CA, USA) and purified in the usual way. They are composed of cationic KRRRKRKRRRKRKRRC and hydrophobic oligo leucine segment with different lengths.

Oligopeptide solutions were analyzed by GPC (Shimadzu Corporation, Kyoto, Japan) which fitted with a combination of two columns of TSK gel G6000PWXL (21.5 mm I.D. × 300 mm length, Tosoh Corporation, Tokyo, Japan) and TSK gel G3000PWXL, RID-10A Refractive index detector, and SPD-M10A UV–VIS detector. Elution was carried out with 1/15 M phosphate buffer (pH 7.5) at 0.3 mL/min.

### 2.2. Critical micelle concentration (CMC) measurements

CMCs of oligopeptides in aqueous solution were measured on a RF5300PC (Shimadzu Corporation, Kyoto, Japan) using pyrene (Nacalai Tesque, Inc., Kyoto, Japan) as a hydrophobic region probe [13]. Five μL of pyrene solution in acetone at a concentration of $6 \times 10^{-5}$ M was transferred into a vial and evaporated. Five hundred μL of oligopeptide solutions which ranging from $5.0 \times 10^{-4}$–1.5 g/L were added dropwise to make the pyrene concentration of $6.0 \times 10^{-7}$ M, incubated at 65 °C for 3 h, and cooled down to the room temperature. Pyrene excitation spectra were measured with the slit widths of 5 and 1.5 nm for excitation and emission at an emission wavelength of 380 nm.

### 2.3. Polyplex formation with pDNA

pCMV-Luc and pT7-Luc (Promega corporation, WI, USA) were amplified to sufficient quantities by standard molecular biology techniques, and purified with a QIAGEN-tip 500 (QIAGEN K.K., Tokyo, Japan). Oligopeptide solutions were mixed with pDNA solutions at a given charge ratio which is the ratio of the number of cationic groups of oligopeptide to that of anionic group of pDNA (*C/A* ratio). The solutions were incubated for 30 min at 37 °C to allow the polyplex formation and analyzed on 0.8 wt% agarose gel in Tris–borate EDTA buffer at 100V for 30 min. pDNA was visualized by staining with 0.5 μg/mL ethidium bromide (EtBr, Sigma chemicals, St Louis, MO, USA).

### 2.4. In vitro *transfection*

COS-1 cells were grown in DMEM (Nissui, Tokyo, Japan) containing 10% fetal bovine serum (FBS) (Sigma chemicals, USA) at 37 °C under a 5% $CO_2$ atmosphere. COS-1 cells were seeded in 96 well culture plates at a density of $1 \times 10^4$ in 100 μL DMEM containing 10% FBS per well. After 24 h incubation, cells were washed with PBS, and 40 μL DMEM was added. Ten μL of polyplex solutions containing 100 ng pCMV-Luc at the concentration above or below CMC of Pep-L12 were poured gently to the wells. Fifty μL of 200 μM chloroquine solution was added (final concentration is 100 μM) and incubated for 5 h. Cells were washed with PBS and cultured for 43 h with DMEM containing 10% FBS at 37 °C in a 5% humidified $CO_2$ environment. The cells were washed with PBS, treated with the lysis buffer containing 1% Triton-X100, and incubated for 30 min at 37 °C. Cell lysate was diluted into luciferase assay solution containing 470 μM luciferin. The relative light units (RLU) of expressed luciferase were measured using ATP-300 Lumicounter (Advantec Toyo Kaisya, Ltd., Tokyo, Japan). Luciferase solutions at a known concentration were used for calibration. The protein concentration was determined by DC Protein Assay kit (Bio-Rad Laboratories, Hercules, CA, USA) using bovine serum albumin as a standard. The obtained luciferase expression (ng luciferase) was divided by total protein content of cell lysates and expressed as ng luciferase/mg protein.

**Table 1**
Sequences of amphiphilic oligopeptides.

| Oligopeptide | Sequences and cleavage sites | Amino acid composition (K/R/L/C) |
|---|---|---|
| Pep-L0 | $H_2N$-K-R-R-R-K-R*-K-R-R*-R-K-R*-K-R-R*-C-$CONH_2$ | 10/5/0/1 |
| Pep-L4 | $H_2N$-$(L)_4$-K-R-R-R-K-R*-K-R-R*-R-K-R*-K-R-R*-C-$CONH_2$ | 10/5/4/1 |
| Pep-L8 | $H_2N$-$(L)_8$-K-R-R-R-K-R*-K-R-R*-R-K-R*-K-R-R*-C-$CONH_2$ | 10/5/8/1 |
| Pep-L12 | $H_2N$-$(L)_{12}$-K-R-R-R-K-R*-K-R-R*-R-K-R*-K-R-R*-C-$CONH_2$ | 10/5/12/1 |

* represents the cleavage site of furin.

### 2.5. Cell-free assay system for luciferase expression

Fifteen μL of polyplexes (*C/A* = 10) were mixed with 12.8 μL of rabbit reticulocyte lysate mixtures ($T_NT$ Coupled Reticulocyte Lysate Systems; Promega, WI, USA) and incubated with shake at rate of 300 rpm/min for 90 min at 30 °C. After transcription/translation assay according to the manufacture's protocol, luciferase activities were measured by the same method described in the above section.

## 3. Results and discussion

### 3.1. Self-assembly of amphiphilic carriers

Sequences and abbreviation of synthesized amphiphilic oligopeptides were shown in Table 1. GPC chart for each amphiphilic oligopeptide in phosphate buffer is shown in Fig. 1. Only Pep-L12 exhibited two peaks, while the other oligopeptides showed peak which is at the similar elution time to the second peak of Pep-L12. The first peak of Pep-L12 is considered to be attributed to the self-assembly of the Pep-L12 with the apparent higher Mw and the second peak corresponds to the unimer as low Mw as the other oligopeptides, Pep-L0, Pep-L4, and Pep-L8. These results indicated that only Pep-L12 forms micelle-like assemblies in aqueous solution.

Micelle-like assemblies can be confirmed by comparing $^1$H NMR spectra in good solvents and water [14,15]. Protons in the core structure composed of the insoluble fractions do not provide sufficient NMR signals. Thus, self-assembly of oligopeptides was analyzed in DMSO and water. Leucine contents ($X_{Leu}$) in water and in DMSO were measured using the signal intensity at 0.8 ppm ($CH_3$ in leucine) and at 1.6 ppm (β-$CH_2$ and γ-CH in leucine, β, γ, and δ-$CH_2$ in lysine, β and γ-$CH_2$ in arginine, and SH in cysteine). The

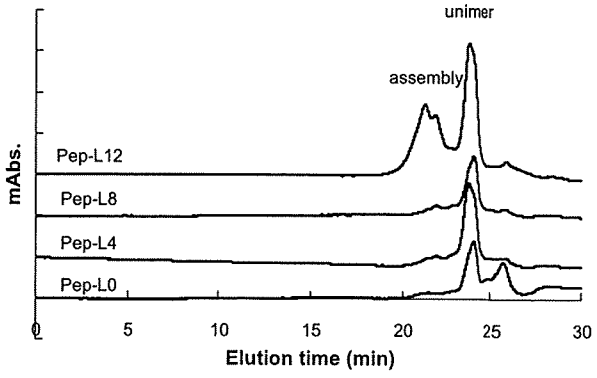


Fig. 1. GPC charts of Pep-LX (*X* = 0, 4, 8 and 12).

relative value of [$X_{Leu}$ in water]/[$X_{Leu}$ in DMSO] for Pep-L4 and Pep-L8 were 1.00 and 1.08, respectively, indicating that these oligopeptides has a same structure in both of medium. On the other hand, [$X_{Leu}$ in water]/[$X_{Leu}$ in DMSO] for Pep-L12 was 0.69, which strongly supports the oligo leucine/oligo cation core/shell structure of Pep-L12 in water.

### 3.2. CMC measurements

The excitation spectra of pyrene in oligopeptides solutions at various concentrations were measured. Fig. 2 demonstrates the intensity ratios ($I_{338.6}/I_{330.4}$) as a function of the logarithm of Pep-L12 concentration. As Pep-L12 concentration increased, the intensity ratio start increasing at a certain concentration, suggesting that pyrene molecules were incorporated into hydrophobic region upon assembly formation. CMC of Pep-L12 is determined from the crossover point was 0.16 g/L. This CMC is very high compared with reported CMC of other amphiphilic polymers [13,16]. This result suggested that Pep-L12 forms unstable assemblies resulting from weak hydrophobic interaction between leucine residues. In case of Pep-L8, a crossover point was not obtained. Hydrophobic interactions of Pep-L8 seem to be not strong enough to form assemblies in aqueous solution, which is in agreed with the GPC chart in Fig. 1. In addition, Pep-L12 assemblies were observed in AFM images above CMC (data not shown). While there were no assemblies at the lower concentration than CMC.

### 3.3. Polyplex formation

Fig. 3 shows the polyplex formation of the Pep-L12 at various *C/A* ratios. When Pep-L12 was mixed with pDNA, bands for free pDNA disappeared at the *C/A* ratio of 5, indicating that all pDNA form polyplexes with carriers. Concentrations of polyplex formation above and below CMC were same, indicating the polyplex forming ability of the micelle-like self-assembly of the Pep-L12 is same to that for Pep-L12 unimer. This phenomenon can be elucidated by the micelle-like architecture, which cationic residues are covering the hydrophobic core. The net amount of the cationic groups was then not significantly changed upon the self-assembly. Pep-L0 also formed polyplexes completely from *C/A* ratio of 5 similar to Pep-L12 (data not shown).

### 3.4. In vitro gene transfection

COS-1 cells were transfected with pCMV-Luc using Pep-L12 and Pep-L0 at various *C/A* ratio, and the transient expressions of

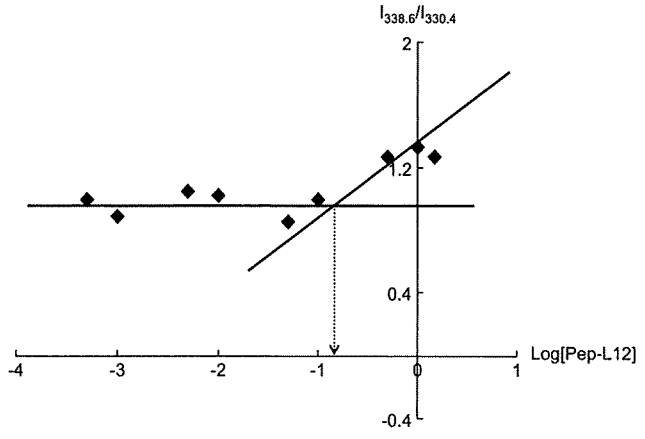


**Fig. 2.** $I_{338.6}/I_{330.4}$ in pyrene excitation spectra versus Pep-L12 concentration. CMC of Pep-L12 was 0.16 g/L.

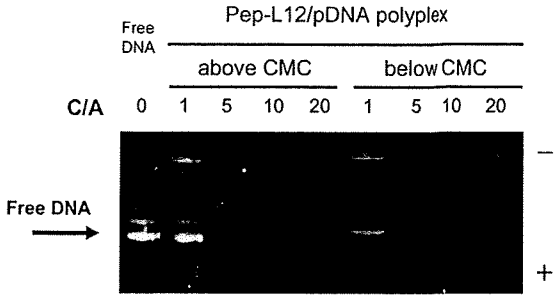


**Fig. 3.** Comparison of electrophoretic mobility profiles of Pep-L12 polyplexes. Polyplexes were analyzed at various *C/A* ratios on an agarose gel (0.8 wt%). Left five lanes represent polyplexes containing 200 ng pDNA above CMC and right four lanes are those containing 100 ng pDNA below CMC.

luciferase gene were evaluated. Cell viabilities for Pep-L12 and Pep-L0 by after transfection procedure were higher than 80% (data not shown). In general, high Mw polycations have profound cell damages, but the cytotoxicity of Pep-L12 above CMC is low. As is shown in Fig. 4(b), both Pep-L0 and Pep-L12 oligopeptides did not work as gene carriers in the unimer forms. However, only Pep-L12 did lead to improved transgene expression as increasing *C/A* ratio when used as the micelle-like architecture above the CMC (Fig. 4(a)). Luciferase expression for Pep-L12 and Pep-L0 was 220.0 ± 68.0 and 19.3 ± 0.2 ng luciferase/mg protein at *C/A* ratio of 10, respectively. Under the same condition, we confirmed that the luciferase expression for oligoarginine (16 mer) was 2.4 ± 0.7 ng luciferase/mg protein at *C/A* ratio of 8 (data not shown). Luciferase expression for Pep-L12 was 100-fold higher than that for widely studied oligoarginine [17], indicating that Pep-L12 is a useful gene carrier.

Possible reasons for improved transfection efficiency by Pep-L12 micell-like carrier is discussed below. First, pDNA uptake was improved because of the high apparent Mw. It was reported that cellular uptakes were increased as increasing in carrier Mw [9,18]. The second reason is the resistance of pDNA to DNase. We have studied the DNase I resistance of polyplexes for poly-L-lysine (from 15 to 1170 mer) or poly-L-arginine (from 70 to 650 mer) by incubating polyplexes with DNase I *in vitro*. As results, higher Mw polypeptide leads to the larger DNase resistance may be because of the large compaction of the polyplexes (data not shown).

Enhanced transcription is the third possible reason for the improved luciferase expression. We previously reported that a micelle-type polycation is superior to the linear-type polycation in gene transfer due to the enhanced transcription [2]. In addition, we found the enhanced gene expression of the linear-type oligopeptide composed of furin cleavage sequences in comparison to control sequences without cleavage sites [12]. These results indicated that the intracellular cleavage of the cationic residues in Pep-L12 self-assembly by intracellular furin enzyme might play a role in weakening the polyplex compaction by decreasing the charge density of the cationic micelle-like architecture.

### 3.5. Transcription/translation efficiency in cell-free system

To elucidate the reason for enhanced transgene expression, cell-free transcription/translation assay was performed using Pep-L0 and Pep-L12. The transcription efficiency of Pep-L12 was suppressed completely in comparison with free pT7-Luc, but Pep-L0 showed slightly residual transcription (Fig. 5). In general, polyplexes composed of high Mw polycation are strongly compacted and then hard to be transcribed. As is similarly, Pep-L12 forming micelle-like structure seems to suppress transcription in cell-free system. However, Pep-L12 successfully led to the transgene

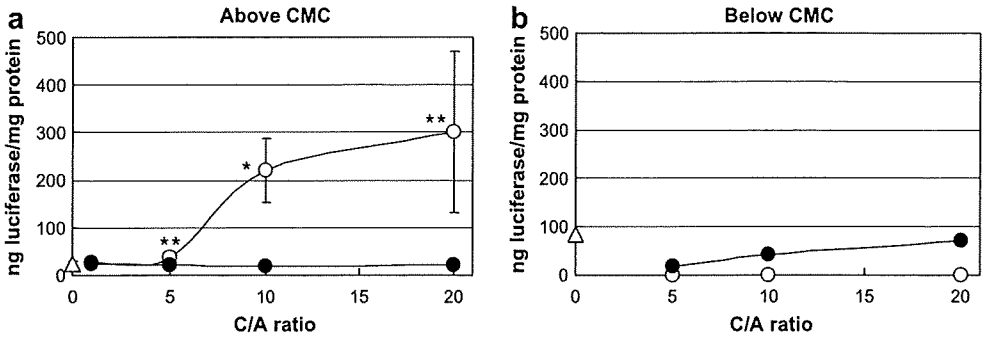


**Fig. 4.** Transient luciferase expression in COS-1 cells transfected using Pep-L0 (●) and Pep-L12 (○) in the presence of 100 μM chloroquine. (△) represents results for naked pCMV-Luc. Transfection assays were perfumed at above (a) or below (b) CMC of Pep-L12. (*$P < 0.01$, **$P < 0.05$.)

expression above CMC when evaluated in COS-1 system (Fig. 4), which indicates that the intracellular furin is able to associate with Pep-L12 somehow in cells.

In the present study, hydrophobic modification of the cationic gene carriers was proved to be effective. Pep-L12 formed hydrophobic/cationic core/shell morphology in aqueous solutions and lead to the enhanced gene expression *in vitro*. This type of core-shell structure should be energetically stable but the inverse structure has been also proposed. Futaki et al. reported that stearylated octaarginine forms polyplexes with the hydrophobic stearyl moieties at the outer surface and induces enhanced transgene expressions due to earlier endosomal escape. They expected that hydrophobic moieties contributed to interactions between polyplexes and cell membranes [19]. In our system, the leucine residues form core structure covered by the charged group and then it worked in the different mechanism.

In order to improve gene delivery efficiency with minimum cytotoxicity, several groups have reported the cross-linking of small PEIs with biodegradable linkage. Linked PEIs presented effective transgene expressions close to or higher than that offered by high Mw PEI (25 kDa) with reduced cytotoxicity [20,21]. Although low Mw PEI is much less cytotoxic than high Mw PEI, undegradable PEI remaining inside cells for a long period of time might interact with cell organelles and affect on cell functions [21]. On the other hand, oligopeptides would be understandably degraded if they remain inside cells after transfection. In this work, we designed novel oligopeptide-type carriers which showed high apparent Mw in aqueous solutions. Synthetic nonviral gene carriers composed of oligopeptides are thought to have potential of low cytotoxicity, enhanced cellular uptake and resistance to DNase. Further researches are necessary to clarify the intracellular behavior, physicochemical properties of polyplexes, such as degree of compaction and surface charge density.

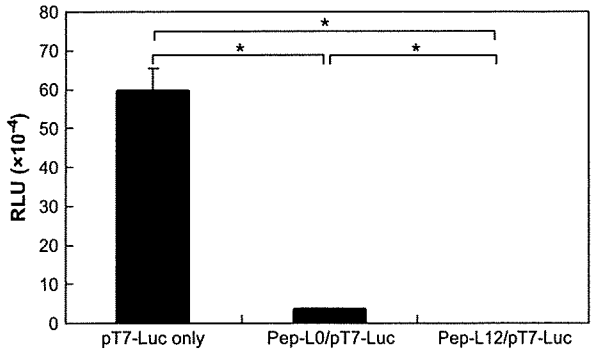


**Fig. 5.** Transcription efficiency determined by luciferase activity in *in vitro* transcription/translation system at *C/A* of 10. Polyplex formation was perfumed at a higher concentration than CMC of Pep-L12. (*$P < 0.0001$.)

## 4. Conclusions

A novel amphiphilic carrier Pep-L12 was synthesized by conjugating cationic sequences and hydrophobic sequences. Pep-L12 formed assemblies in aqueous solution at concentration above 0.16 g/L. Formations of assemblies brought about a dramatic increasing apparent Mw of carriers. Assemblies led enhanced transgene expression than linear carriers. Further analysis has to be done to design more effective self-assembly type gene carrier with low cytotoxicity.

## Acknowledgements

We thank to Prof. Osam Mazda of Kyoto Prefectural University of Medicine for his great suggestion. This work was partly supported by Grants for Regional Science and Technology Promotion from the Ministry of Education, Culture, Sports, Science and Technology.

## References

[1] Kimura T, Yamaoka T, Iwase R, Murakami A. Effect of physicochemical properties of polyplexes composed of chemically modified PL derivatives on transfection efficiency in vitro. Macromol Biosci 2002;2:437–46.
[2] Kitagawa T, Iwase R, Ishihara K, Yamaoka T, Murakami A. Facilitated disassembly of polyplexes composed of self-assembling amphiphilic polycations enhances the gene transfer efficacy. Chem Lett 2005;34(11):1478–9.
[3] Honore I, Grosse S, Frison N, Favatier F, Monsigny M, Fajac I. Transcription of plasmid DNA: influence of plasmid DNA/polyethylenimine complex formation. J Control Release 2005;107(3):537–46.
[4] Schaffer DV, Fidelman NA, Dan N, Lauffenburger DA. Vector unpacking as a potential barrier for receptor-mediated polyplex gene delivery. Biotechnol Bioeng 2000;67(5):598–606.
[5] Godbey WT, Wu KK, Mikos AG. Size matters: molecular weight affects the efficiency of poly(ethylenimine) as a gene delivery vehicle. J Biomed Mater Res 1999;45(3):268–75.
[6] Kunath K, VH A, Fischer D, Petersen H, Bickel U, Voigt K, et al. Low-molecular-weight polyethylenimine as a non-viral vector for DNA delivery: comparison of physicochemical properties, transfection efficiency and in vivo distribution with high-molecular-weight polyethylenimine. J Control Release 2003;89(1):113–25.
[7] Breunig M, Lungwitz U, Liebl R, Fontanari C, Klar J, Kurtz A, et al. Gene delivery with low molecular weight linear polyethylenimines. J Gene Med 2005;7(10):1287–98.
[8] Bettinger T, Carlisle RC, Read ML, Ogris M, Seymour LW. Peptide-mediated RNA delivery: a novel approach for enhanced transfection of primary and post-mitotic cells. Nucleic Acids Res 2001;29(18):3882–91.
[9] Varga CM, Tedford NC, Thomas M, Klibanov AM, Griffith LG, Lauffenburger DA. Quantitative comparison of polyethylenimine formulations and adenoviral vectors in terms of intracellular gene delivery processes. Gene Ther 2005; 12(13):1023–32.
[10] Hosaka MNM, Kim WS, Watanabe T, Hatsuzawa K, Ikemizu J, Murakami K, et al. Arg-X-Lys/Arg-Arg motif as a signal for precursor cleavage catalyzed by furin within the constitutive secretory pathway. J Biol Chem 1991;266(19):12127–30.

[11] Molloy SSBP, Leppla SH, Klimpel KR, Thomas G. Human furin is a calcium-dependent serine endoprotease that recognizes the sequence Arg-X-X-Arg and efficiently cleaves anthrax toxin protective antigen. J Biol Chem 1992;267(23): 16396–402.
[12] Hashimoto T, Tachibana Y, Nozaki H, Mazda O, Niidome T, Murakami A, et al. Intracellular enzyme-responsive fragmentation of nonviral gene carriers leads to polyplex destabilization and enhanced transgene expression. Chem Lett, in press.
[13] Lee KY, Kwon IC, Kim YH, Jo WH, Jeong SY. Preparation of chitosan self-aggregates as a gene delivery system. J Control Release 1998;51(2–3):213–20.
[14] Liu M, Kono K, Frechet JMJ. Water-soluble dendritic unimolecular micelle: their potential as drug delivery agents. J Control Release 2000;65(1–2):121–31.
[15] Jette KK, Law D, Schmitt EA, Kwon GS. Preparation and drug loading of poly(ethylene glycol)-block-poly(ε-caprolactone) micelles through the evaporation of a cosolvent azeotrope. Pharm Res 2004;21(7):1184–91.
[16] Zhang J, Wang LQ, Wang H, Tu K. Micellization phenomena of amphiphilic block copolymers based on methoxy poly(ethylene glycol) and either crystalline or amorphous poly(caprolactone-b-lactide). Biomacromolecules 2006;7(9):2492–500.
[17] Fuchs SM, Raines RT. Pathway for polyarginine entry into mammalian cells. Biochemistry 2004;43(9):2438–44.
[18] Wender PA, Mitchell DJ, Pattabiraman K, Pelkey ET, Steinman L, Rothbard JB. The design, synthesis, and evaluation of molecules that enable or enhance cellular uptake: peptoid molecular transporters. Proc Natl Acad Sci U S A 2000;97(24):13003–8.
[19] Futaki S, Ohashi W, Suzuki T, Niwa M, Tanaka S, Ueda K, et al. Stearylated arginine-rich peptides: a new class of transfection systems. Bioconjug Chem 2001;12(6):1005–11.
[20] Thomas M, Ge Q, Lu JJ, Chen J, Klibanov AM. Cross-linked small polyethylenimines: while still nontoxic, deliver DNA efficiently to mammalian cells in vitro and in vivo. Pharm Res 2005;22(3):373–80.
[21] Tang GP, Guo HY, Alexis F, Wang X, Zeng S, Lim TM, et al. Low molecular weight polyethylenimines linked by beta-cyclodextrin for gene transfer into the nervous system. J Gene Med 2006;8(6):736–44.

Acta Biomaterialia xxx (2009) xxx–xxx

Contents lists available at ScienceDirect

Acta Biomaterialia

journal homepage: www.elsevier.com/locate/actabiomat

# Stable modification of poly(lactic acid) surface with neurite outgrowth-promoting peptides via hydrophobic collagen-like sequence

Sachiro Kakinoki, Tetsuji Yamaoka *

*Department of Biomedical Engineering, National Cardiovascular Center Research Institute, 5-7-1 Fujishirodai, Suita, Osaka 565-8565, Japan*
*JST, CREST, 5 Sanbancho, Chiyoda-ku, Tokyo 102-0075, Japan*

ARTICLE INFO

*Article history:*
Received 30 July 2009
Received in revised form 11 November 2009
Accepted 1 December 2009
Available online xxxx

*Keywords:*
Surface modification
PLA scaffold
Peptide adsorption
Hydrophobic interaction
Neurite outgrowth-promoting peptide

ABSTRACT

Surface modification of poly(DL-lactic acid) (PLA) scaffolds has been performed using a biofunctional small peptide composed of collagen-like repetitive sequence and laminin-derived sequence (AG73-$G_3$-$(PPG)_5$) via hydrophobic interaction. The results of surface analysis suggest that AG73-$G_3$-$(PPG)_5$ can be stably adsorbed onto PLA films via hydrophobic interaction at the $(PPG)_5$ region, and form an extracellular matrix-like layer composed of both structural and biosignalling sequences. In addition, neurite outgrowth of PC12 cells was observed on the AG73-$G_3$-$(PPG)_5$-adsorbed PLA film. These results indicate that AG73-$G_3$-$(PPG)_5$ very effectively enhances neurite outgrowth activity on PLA films. The hydrophobic adsorption of collagen-like peptide bound to biosignalling molecules may be widely applied as a surface modifier of PLA films for tissue engineering.



## 1. Introduction

Tissue engineering has been proposed as an approach to replace damaged, injured or missing tissue with biologically compatible substrate combining cells or biosignalling molecules and scaffolds [1,2]. Scaffolds assume the role of a temporary extracellular matrix (ECM) where biodegradability and biocompatibility are essential for tissue regeneration. Furthermore, biodegradable scaffolds should be designed not to obstruct tissue regeneration via cell-induced natural healing. The cellular responses to the scaffold surfaces determine whether tissue regeneration will be promoted or obstructed. Therefore, it is very important to control the biological property of the scaffold surfaces [3].

Poly(lactic acid) (PLA) is widely used for biodegradable scaffolds as it possesses a number of suitable characteristics for this role. PLA can be hydrolytically degraded into lactic acid; this degradation requires only water, and the final product can immediately be metabolized in vivo [4]. Moreover, PLA material exhibits excellent shaping and molding properties because of its mechanical versatility. However, insufficient interaction between PLA materials and cells leading to in vivo foreign-body reactions is a major problem because the required biological activities are not inherent in PLA. PLA lacks functional groups and so cannot be easily modified with bioactive molecules. Therefore, many investigators have attempted to impart functional groups to PLA in order to enhance its biological activity by using copolymerization or chemical grafting with other polymers [5], plasma treatment [6], chemical modification [7] and physical adsorption. In previous studies, we reported on the preparation of poly(lactic-co-malic acid)-conjugated Arg-Gly-Asp (RGD) tripeptide [8] and gelatin-immobilized PLA scaffold [9] in order to improve the cell attachment. However, because these techniques are prone to adverse chemical reactions, it is necessary to develop techniques that are simpler and offer better biocompatibility. Physical adsorption, which is driven by electrostatic, hydrophobic and specific interactions, has been noted as a simpler surface modification technique of PLA scaffolds [10–12].

In the current work, neurite outgrowth-promoting peptides, consisting of laminin-derived sequence and collagen-like sequence, were designed as surface modifiers of PLA films via hydrophobic adsorption. PLA is preferred as a base material for a nerve regeneration conduit because of its excellent shaping and molding properties [13]. However, PLA does not inherently cater to any nerve regeneration activity. If biologically modified PLA-based artificial nerve can promote nerve regeneration, it might be possible to avoid donor site defects in autologous nerve transplantation. It was reported that laminin-derived sequence AG73 supports neurite outgrowth [14], and therefore was selected as a nerve-regenerating peptide.

On the other hand, it is well known that collagen is a predominant component of ECM [15,16]. The major part of collagen

* Corresponding author. Address: Department of Biomedical Engineering, National Cardiovascular Center Research Institute, 5-7-1 Fujishirodai, Suita, Osaka 565-8565, Japan. Tel.: +81 6 6833 5012x2637; fax: +81 6 6835 5476.
*E-mail address:* yamtet@ri.ncvc.go.jp (T. Yamaoka).

1742-7061/$ - see front matter © 2009 Acta Materialia Inc. Published by Elsevier Ltd. All rights reserved.
doi:10.1016/j.actbio.2009.12.001

consists of Xaa-Yaa-Gly repetitive sequences, where Xaa and Yaa positions are often occupied by Pro and 4(R)-hydroxyproline (Hyp), respectively, and forms the hydrophobic polyproline-II (PP-II) structure [17–20]. The collagen triple-helix structure is composed of three PP-II chains, and collagen-like peptides (CLPs) such as $(Pro\text{-}Pro\text{-}Gly)_n$ are also able to form a triple-helix structure [21–23]; therefore, CLP is expected to be adsorbed by PLA films via hydrophobic interaction. Animal-derived collagen has also been intensively investigated as a conduit for nerve regeneration because of its high bioactivity [24]. However, animal-derived collagens possess high antigenicity in vivo because of the unnecessary biosignal sequences and enzymatically digested fragments [25]. CLP, which is the repetitive sequence at a structural region of collagen without any enzyme-digestible sequence, is anticipated to be of low immunogenicity.

Here, we are reporting on a neurite outgrowth-promoting peptide composed of AG73 and CLP (AG73-$G_3$-$(PPG)_5$) as a surface modifier of PLA films for tissue engineering. Conformation of AG73-$G_3$-$(PPG)_5$ was studied by circular dichroism (CD) spectroscopy. The surface characteristics of AG73-$G_3$-$(PPG)_5$-adsorbed PLA film were investigated by water contact angle measurement and X-ray photoelectron spectroscopy (XPS). PC12 cells were primed with nerve growth factor (NGF) and cultured on the AG73-$G_3$-$(PPG)_5$-adsorbed PLA films, and the neurite outgrowth activity was then quantified.

## 2. Materials and methods

### 2.1. Materials

$(PPG)_{10}$, AG73 (RKRLQVQLSIRT) and AG73-$G_3$-$(PPG)_5$ were commercially synthesized by SCRUM, Inc. (Tokyo, Japan). PLA (Mw 130,000) was obtained from Mitsui Chemicals, Inc. (Tokyo, Japan). Progesterone, sodium selenite ($N_2SeO_3$) and transferrin were purchased from Nacalai Tesque, Inc. (Kyoto, Japan). NGF and horse serum (HS) were obtained from Sigma–Aldrich, Inc. (St. Louis, MO, USA). Insulin, advanced DMEM/F12 and penicillin–streptomycin were purchased from Invitrogen Corporation (Carlsbad, CA, USA). Fetal bovine serum (FBS) was obtained from MP Biomedicals, Inc. (Solon, OH, USA).

### 2.2. Methods

#### 2.2.1. Circular dichroism

CD spectra were measured by a J-720 spectropolarimeter (Jasco Co., Tokyo, Japan) with a standard analysis program. The temperature was controlled using a recirculating waterbath and spectra was recorded with a 0.1 cm path length cell, using a scanning speed 10 nm $min^{-1}$, with a 1.0 nm spectral bandwidth, over the wavelength range from 190 to 250 nm. Peptides were dissolved with water at 0.25 mM. Data are represented in molar elipticities ($[\theta]$ deg $cm^2$ $dmol^{-1}$).

#### 2.2.2. Peptide adsorption on PLA films

PLA films (diameter $\varphi = 6.0$ mm; $t = 0.5$ mm) were prepared with a hot shrinking machine at 180 °C and sterilized by UV irradiation. Three peptides, $(PPG)_{10}$, AG73, and AG73-$G_3$-$(PPG)_5$, were dissolved in sterilized water at 10 μM, and then 1 ml of each peptide solution was poured onto a PLA film in a 24-well cell culture plate. Peptide solutions were dried for 24 h. In order to get rid of any excessively adsorbed peptide, the PLA films were washed with 1 ml of sterilized $H_2O$ or 1.0 M NaCl aqueous solution twice for 30 min, and then the films were washed with 1 ml of sterilized $H_2O$ again and dried in vacuo.

#### 2.2.3. Water contact angle

The contact angle with distilled water was measured by using a contact-angle meter (CA-X; Kyowa Interface Science Co., Ltd., Saitama, Japan). Images of the water spreading on the sample were recorded by a camera and then analyzed. Three samples were measured for each group.

#### 2.2.4. X-ray photoelectron spectroscopy

The surface composition of peptide-adsorbed PLA films was determined using an ESCA-3400 (Shimadzu Co., Kyoto, Japan). The X-ray source was a monochromatic Mg $K_\alpha$ X-ray from a rotating anode. Survey scans were measured from 0 to 1200 eV. Peak positions and areas were analyzed and ratios for C1s, N1s and O1s were calculated by using software provided by the manufacturer.

### 2.3. Cell culture

Rat adrenal pheochromocytoma PC12 cells (RIKEN BioResource Center, Ibaraki, Japan) were maintained in DMEM supplemented with 100 U $ml^{-1}$ penicillin, 100 μg $ml^{-1}$ streptomycin, 10% FBS and 7.5% HS. PC12 cells were cultured in poly-D-Lys coated cell-culture dishes (BD, NJ, USA) and maintained at 37 °C in an atmosphere of 5% $CO_2$ and 95% air.

### 2.4. Neurite outgrowth assay

The neurite outgrowth assay was performed by using PC12 cells as the model of neural stem cells [26]. PC12 cells were primed with 100 ng $ml^{-1}$ NGF for 24 h on polystyrene cell-culture dishes. The cells were then collected by agitation and placed in the culture medium for 30 min at 37 °C in an atmosphere of 5% $CO_2$ and 95% air. The cells were washed and resuspended with advanced DMEM/F12 containing 5 μg $ml^{-1}$ insulin, 100 ng $ml^{-1}$ NGF, 20 nM progesterone, 30 nM $Na_2SeO_3$ and 100 mg $ml^{-1}$ transferrin. The cells were then seeded on peptide-adsorbed PLA films at a seeding density of $2.0 \times 10^4$ cells $film^{-1}$ in 24-well cell culture plates, and incubated at 37 °C for 24 h. PC12 cells on peptide-adsorbed PLA films were fixed with 10% formalin and stained by 4% crystal violet/methanol solution, and then the number of PC cells with or without neurites was determined in order to evaluate the neurite outgrowth activity as described elsewhere [27,28]. The lengths of neurites were measured using software (Image J; National Institute of Mental Health, MD, USA) [29]. Cells with neurites longer than 50 μm and those with neurites shorter than 50 μm were counted separately.

## 3. Results and discussion

### 3.1. Secondary structure of peptides

The CD spectra of $(PPG)_{10}$, AG73 and AG73-$G_3$-$(PPG)_5$ are shown in Fig. 1. The CD spectrum of $(PPG)_{10}$ in water at 37 °C exhibited a strong negative band at 209 nm and a positive band at 229 nm, which are known as typical patterns of collagen triple-helix and PP-II structure [20,30]. Although the CD spectrum of PP-II is similar to that of collagen triple-helix, the transition temperature of $(PPG)_{10}$ is reported to be about 28 °C in water [31]. Therefore, this CD spectrum indicates that $(PPG)_{10}$ forms the PP-II structure. The CD spectrum of AG73 showed a strong negative band at 199 nm, assigned as a random-coil structure. In the case of AG73-$G_3$-$(PPG)_5$, the CD spectrum indicated an intermediate pattern between $(PPG)_{10}$ and AG73. This means that a negative band was blue-shifted and a positive band at 229 nm was decreased in comparison with $(PPG)_{10}$. In addition, all CD spectra have an isosbestic

Please cite this article in press as: Kakinoki S, Yamaoka T. Stable modification of poly(lactic acid) surface with neurite outgrowth-promoting peptides via hydrophobic collagen-like sequence. Acta Biomater (2009), doi:10.1016/j.actbio.2009.12.001